# Electrophysiologic effects of acute myocardial ischemia: a theoretical study of altered cell excitability and action potential duration [1]

Robin M. Shaw, Yoram Rudy *

*Cardiac Bioelectricity Research and Training Center, Department of Biomedical Engineering, Case Western Reserve University, Cleveland, OH 44106-7207, USA*

## Abstract

**Objective**: To study the ionic mechanisms of electrophysiologic changes in cell excitability and action potential duration during the acute phase of myocardial ischemia. **Methods**: Using an ionic-based theoretical model of the cardiac ventricular cell, the dynamic LRd model, we have simulated the three major component conditions of acute ischemia (elevated $[K]_o$, acidosis and anoxia) at the level of individual ionic currents and ionic concentrations. The conditions were applied individually and in combination to identify ionic mechanisms responsible for reduced excitability at rest potentials, delayed recovery of excitability, and shortened action potential duration. **Results:** Increased extracellular potassium ($[K]_o$) had the major effect on cell excitability by depolarizing resting membrane potential ($V_{rest}$), causing reduction in sodium channel availability. Acidosis caused a $[K]_o$-independent reduction in maximum upstroke velocity, $(dV_m/dt)_{max}$. A transition from sodium-current dominated to calcium-current dominated upstroke occurred, and calcium current alone was able to sustain the upstroke, but only after sodium channels were almost completely (97%) inactivated. Acidic conditions prevented the transition to calcium dominated upstroke by acidic reduction of both sodium and calcium currents. Anoxia, simulated by lowering $[ATP]_i$ and activating the ATP-dependent potassium current, $I_{K(ATP)}$, was the only process that could decrease action potential duration by more than 50% and reproduce AP shape changes that are observed experimentally. Acidic or anoxic depression of the L-type calcium current could not reproduce the observed action potential shape changes and APD shortening. Delayed recovery of excitability, known as 'post-repolarization refractoriness', was determined by the voltage-dependent kinetics of sodium channel recovery; $V_{rest}$ depolarization caused by elevated $[K]_o$ increased the time constant of $(dV_m/dt)_{max}$ recovery from $\tau = 10.3$ ms at $[K]_o = 4.5$ mM to $\tau = 81.4$ ms at $[K]_o = 12$ mM, reflecting major slowing of sodium-channel recovery. Anoxia and acidosis had little affect on $\tau$. **Conclusions**: The major conditions of acute ischemia, namely elevated $[K]_o$, acidosis and anoxia, applied at the ionic channel level are sufficient to simulate the major electrical changes associated with ischemia. Depression of membrane excitability and delayed recovery of excitability in the single, unloaded cell are caused by elevated $[K]_o$ with additional excitability depression by acidosis. Major changes in action potential duration and shape can only be accounted for by anoxia-dependent opening of $I_{K(ATP)}$. © 1997 Elsevier Science B.V.

*Keywords:* Myocardial ischemia; Hyperkalemia; Acidosis; Anoxia; Membrane excitability; Action potential duration; Potassium channel, ATP sensitive; Computer model

## 1. Introduction

The major pathophysiological component conditions of acute myocardial ischemia are elevated extracellular potassium ($[K]_o$), acidosis, and anoxia. These conditions cause the following electrical changes: reduction in membrane excitability, shortening of action potential duration (APD), and prolongation of recovery of excitability following an action potential [1–3]. Difficulties exist in determining the ionic mechanisms of the electrical changes, and the contribution of each pathophysiological condition to each electrical change. We have attempted to relate the electrical changes to the component conditions and to determine the ionic mechanisms, using a detailed theoretical model of

---

* Corresponding author. Tel. +1 216 368-4051; Fax +1 216 368-4969.
[1] Previously published in abstract form (*Biophysical Journal* 1997;72:A47).

acute myocardial ischemia. The model was developed by separately simulating the effects of each pathophysiological condition on individual ion-channel currents in a dynamic mathematical model of the cardiac ventricular action potential (the LRd model) [4–6]. A theoretical model allows pathophysiological conditions to be selectively evaluated so that mechanisms can be examined at the specific ionic current and channel level.

The broad experimental literature has generated extensive data on the ionic mechanisms associated with ischemic electrophysiologic changes. Membrane excitability and the action potential upstroke are typically determined by the fast sodium current ($I_{Na}$) [7]. In highly depressed ischemic tissue, calcium current ($I_{Ca(L)}$) plays a role in the upstroke [8,9], and may even dominate action potential generation [10]. We are interested in the conditions that affect a transition from an $I_{Na}$-controlled upstroke to an $I_{Ca(L)}$-controlled upstroke.

Beyond the upstroke, APD is reduced by enhancement of the ATP-dependent potassium current ($I_{K(ATP)}$) [11]. Other putative mechanisms of shortening include enhancement of outward potassium currents secondary to elevated $[K]_o$ and acidic and anoxic reduction of $I_{Ca(L)}$. Following an action potential, membrane excitability normally recovers upon return to resting membrane potential, $V_{rest}$. Ischemic conditions can cause postrepolarization refractoriness [12,13], extending membrane refractoriness hundreds of milliseconds beyond the return to $V_{rest}$. Elevated $[K]_o$ has been identified as the principal pathophysiological condition associated with postrepolarization refractoriness. Hypoxia at elevated $[K]_o$ has been associated with aggravating the postrepolarization refractoriness phenomenon [14], but the mechanism is not clear. In this study, we attempt to determine the relative contribution of each ischemic condition to APD shortening and delayed recovery of excitability.

Mapping experiments have shown that reentrant arrhythmias occur during the first 2–10 min of acute ischemia [2,15,16]. The studies contained here explore the mechanisms of altered excitability and action potential duration, which are important parameters in the initiation and sustenance of reentry. The mechanistic insights obtained, together with theoretical studies of action potential conduction [17] and the extensive information that is available from experimental observations, can provide a basis for a mechanistic approach to the treatment of fatal arrhythmias associated with acute myocardial ischemia.

## 2. Methods

### 2.1. Ventricular cell model

The dynamic LRd model is a general mammalian ventricular cell model, based mainly on data taken from the guinea-pig. Included in the model are the membrane ionic channel currents, represented mathematically by a Hodgkin–Huxley type formalism, as well as ionic pumps
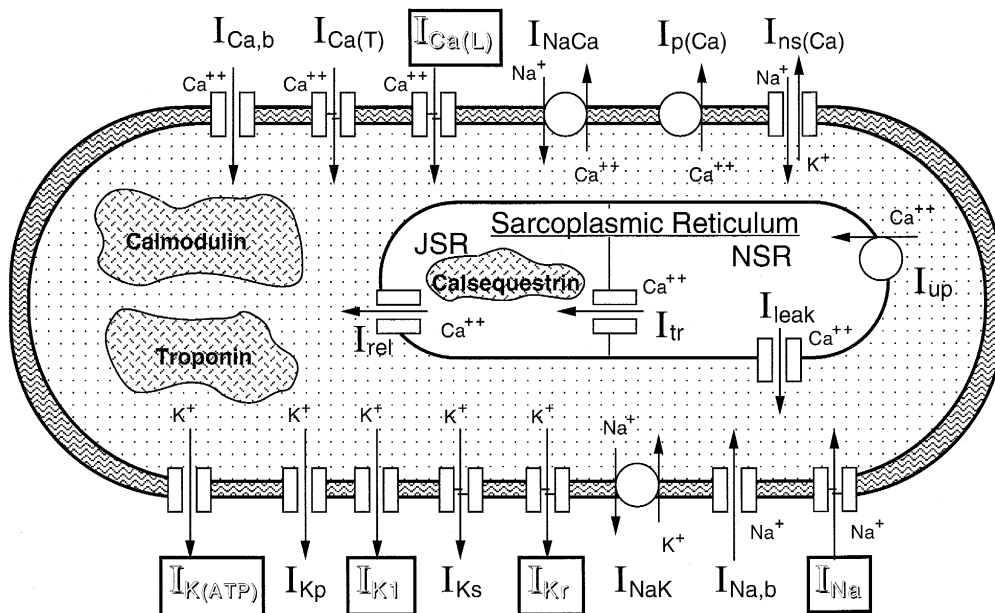


Fig. 1. Schematic diagram of the LRd ventricular cell model. Processes affected by the simulated ischemic conditions are identified by rectangular frames. $I_{Na}$, fast sodium current; $I_{Ca(L)}$, calcium current through L-type calcium channels; $I_{Ca(T)}$, calcium current through T-type calcium channels; $I_{Kr}$, fast component of the delayed rectifier potassium current; $I_{Ks}$, slow component of the delayed rectifier potassium current; $I_{K1}$, inward rectifier potassium current; $I_{Kp}$, plateau potassium current; $I_{K(ATP)}$, ATP sensitive potassium current; $I_{NaK}$, sodium–potassium pump current; $I_{NaCa}$, sodium–calcium exchange current; $I_{p(Ca)}$, calcium pump in the sarcolemma; $I_{Na,b}$, sodium background current; $I_{Ca,b}$, calcium background current; $I_{ns(Ca)}$, nonspecific calcium-activated current; $I_{up}$, calcium uptake from the myoplasm to network sarcoplasmic reticulum (NSR); $I_{rel}$, calcium release from junctional sarcoplasmic reticulum (JSR); $I_{leak}$, calcium leakage from NSR to myoplasm; $I_{tr}$, calcium translocation from NSR to JSR. For details see references [4–6].

and exchangers. In addition, processes that regulate ionic concentration changes, especially dynamic changes of intracellular calcium, are introduced. The model includes the recent development [6] to account for the two components of the delayed rectifier potassium current, $I_{Kr}$ and $I_{Ks}$. A diagram of the cell model is provided in Fig. 1 where processes altered by the simulated ischemic conditions are identified by rectangular frames. Detailed tables of equations governing the model are provided in References [4–6].

The ionic and metabolic conditions of ischemia have been approached as three different entities: (1) increase in extracellular potassium, (2) intracellular and extracellular acidosis, and (3) anoxia and metabolic blockade. The approach and theoretical implementation of each condition is presented in our study of conduction in an ischemic fiber [17], summarized in Appendix A, and discussed briefly below.

## 2.2. Increased extracellular potassium concentration, $[K]_o$

Experimentally, $[K]_o$ undergoes a triphasic change (increase to about 10 mM, plateau, and secondary increase) during the first 15 min of acute ischemia [18,19]. In our simulations we examine the range of extracellular potassium concentrations that occur during the triphasic change (4–20 mM). We assign a value of $[K]_o$, analogous to the experimental technique of perfusing the tissue with a constant $[K]_o$. Elevated $[K]_o$ directly enhances the conductances of $I_{K1}$ (proportional to $[K]_o^{1/2}$) [4], $I_{Kr}$ (proportional to $[K]_o^{1/2}$) [6], and $I_{K(ATP)}$ (proportional to $[K]_o^{0.24}$, see below). In addition, the potassium reversal potential ($E_K$) is less negative and $I_{NaK}$ is augmented in the direction of $Na^+$ extrusion (an electrogenic outward current).

## 2.3. Acidosis

Intracellular and extracellular pH drop linearly with time during the first 10 min of acute ischemia, reaching at the 10 min mark a level about 1 pH unit below their normal value [2,20]. Yatani et al. [21] observed in a study with rat ventricular cells that low extracellular pH both decreased maximum sodium current and shifted the sodium channel current-voltage curves to the right (i.e., to more positive potentials). In studies with guinea-pig ventricular tissue, Kagiyama et al. [22] found that a one unit drop in pH decreases the maximum conductance of $I_{Na}$ by 25%, and shifts its voltage dependence by 3.4 mV ($I_{Na}$ was assessed by recording maximum upstroke velocity of the action potential). Since the LRd mammalian ventricular cell model is based mostly on guinea-pig studies, we incorporated the specific effects of acidosis as noted by Kagiyama et al. [22].

Similar to the effect on the sodium current, acidosis reduces the magnitude of the L-type calcium current. Irisawa and Sato [23] found, for guinea-pig ventricular

cells, a sigmoidal decrease in conductance (50% at pH = 6.6) upon intracellular acidosis and no significant response to extracellular acidosis. They did not find a shift in the calcium current-voltage curves, and concluded that acidosis has no significant effect on calcium channel kinetics. We simulate the effects of acidosis on calcium current by reducing its maximum conductance, $\bar{I}_{Ca(L)}$, by up to 50%.

Independent of the above effects, acidosis also causes a 2–5 mV depolarization of resting membrane potential [1,24], $V_{rest}$. The most likely cause of $V_{rest}$ changes (independent of $[K]_o$) is a decrease in intracellular potassium concentration, $[K]_i$ [18,25]. Our acidic condition includes a decrease in $[K]_i$ from 144.8 to 125 mM, which results in a 3.8 mV depolarization of $V_{rest}$.

## 2.4. Anoxia

Many experimental protocols are conducted under conditions of hypoxia rather than complete anoxia. We model the consequences of abrupt and complete cessation of perfusion, and therefore refer to our simulation protocol as anoxia. The direct effects of anoxia are linked to its detrimental effect on cellular respiration and consequent decrease in ATP availability. In 1983, Noma reported a specific ATP-sensitive potassium channel ($I_{K(ATP)}$) that is inactive in healthy ventricular tissue and is increasingly outward with decreasing levels of ATP [26]. $I_{K(ATP)}$ does not vary with time or voltage. Our formulation of $I_{K(ATP)}$, originally formulated in Reference [27], is

$$I_{K(ATP)} = \bar{g}_{K(ATP)} \cdot P_{ATP} \cdot ([K]_o/4.0)^n \cdot (V_m - E_K) \quad (2)$$

where $\bar{g}_{K(ATP)}$ is maximum channel conductance per unit capacitative membrane area (nS/$\mu$F) at 0 mM $[ATP]_i$. Nichols et al. [28] determined $\bar{g}_{K(ATP)}$ of 195 nS/cell in whole cell guinea-pig recordings at $[K]_o = 4.0$ mM and physiologic concentrations of ADP, GDP and free $Mg^{2+}$. The Nichols et al. [28] data adjusted to LRd cell size are used for single channel conductance estimates. In the LRd cell model which is 100 $\mu$m in length and 11 $\mu$m in diameter, $\bar{g}_{K(ATP)} = 4$ mS/$\mu$F. This conductance is on the same order as maximum sodium channel conductance, $\bar{g}_{Na} = 16$ mS/$\mu$F. $P_{ATP}$ is the percentage availability of $I_{K(ATP)}$ channels at a given ATP concentration. $P_{ATP}$ has sigmoidal dependence [28,29] on $[ATP]_i$ and can be expressed with Hill-type formalism with a half-maximal saturation point ($k_{1/2}$, mM), and Hill coefficient ($H$). Nichols et al. [28] determined $k_{1/2} = 114$ $\mu$M and $H = 2$. Metabolic factors present during acute ischemia decrease $I_{K(ATP)}$ sensitivity to $[ATP]_i$-based inactivation (increase $k_{1/2}$). These factors include ADP which was present in the Nichols et al. [28] preparation, intracellular acidosis [30] (2 $\times$ increase in $k_{1/2}$) and intracellular lactate [31] (3 $\times$ increase in $k_{1/2}$). We modified $k_{1/2}$ to 250 $\mu$M to account for these additional ischemic effects. $P_{ATP}$ reproduces with good accuracy the dependence of $I_{K(ATP)}$ on

[ATP]$_i$, as shown in Fig. 2A. In addition to $P_{ATP}$, conductance through $I_{K(ATP)}$ is a function of [K]$_o$ (similar to the $I_{K1}$ and $I_{Kr}$ conductances). This dependence is to the power of $n = 0.24$ in the guinea-pig ventricular cell [32]. Fig. 2B and 2C correspond to our theoretically formulated (2B) and to the measured [32] (2C) single channel current-voltage curves at [ATP]$_i$ = 0 mM and [K]$_o$ = 5.4, 50 and 150 mM. In Fig. 2B, whole cell currents are converted to single channel currents by assuming a channel density of 1.36 channels/$\mu$m$^2$. $I_{K(ATP)}$ channel density has been estimated from single patch data to be about three times

higher [28,29], and thus our formulation of $I_{K(ATP)}$ corresponds to a conservative estimate.

In addition to $I_{K(ATP)}$, ATP-dependence of the L-type calcium channel has been introduced into the model. Noma and Shibasaki [33] recorded the dependence of $I_{Ca(L)}$ on [ATP]$_i$ using guinea-pig ventricular cells. We used a Hill-type fit, $k_{1/2} = 1.4$ mM and $H = 2.6$, to the Noma and Shibasaki [33] data for metabolic regulation of $I_{Ca(L)}$. These parameters cause 12% $I_{Ca(L)}$ reduction at [ATP]$_i$ = 3 mM, very similar to the reduction of $I_{Ca(L)}$ recorded by Ohya and Sperelakis [34] using vascular smooth muscle
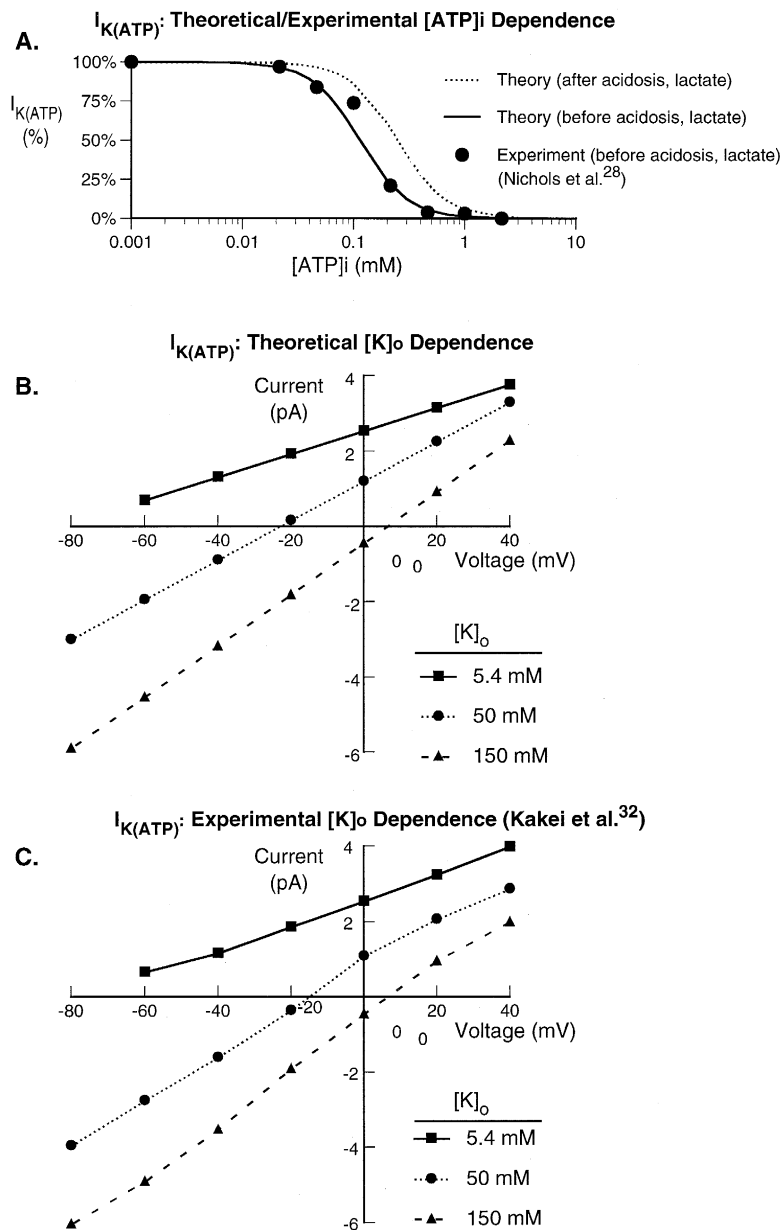


Fig. 2. $I_{K(ATP)}$ dependence on [ATP]$_i$ and [K]$_o$. (A) Sigmoidal dependence of (normalized) $I_{K(ATP)}$ on [ATP]$_i$. [K]$_o$ held constant at 4.0 mM. Filled circles are measured data by Nichols et al. [28], solid line is the theoretical curve and dashed line is the modified theoretical curve that accounts for acidosis and lactate. (B) Computed single channel current-voltage curves of $I_{K(ATP)}$ for three different values of [K]$_o$ at [ATP]$_i$ = 0.0 mM. (C) Measured single channel current-voltage curves of guinea-pig $I_{K(ATP)}$ (Kakei et al. [32]) under similar conditions as in (B).

cells at similar $[ATP]_i$. The complete formulation of $I_{K(ATP)}$, ATP-dependence of $I_{Ca(L)}$, and associated parameters are provided in Appendix A.

### 2.5. Protocols and definitions

Transmembrane currents are computed using the modified Euler method of Rush and Larsen [35] with a constant time step of 2 $\mu$S. The cell is excited with a 0.5 ms intracellular current stimulus of $-80$ $\mu$A/$\mu$F, unless otherwise specified. $(dV_m/dt)_{max}$ is always the largest slope computed during the entire upstroke, not a local maximum. Action potential duration, $APD_{90}$, is the time between $(dV_m/dt)_{max}$ and 90% repolarization from peak amplitude (peak potential minus resting potential). Control $[K]_o$ is 4.5 mM.

## 3. Results

### 3.1. Resting membrane potential

The majority of increased $[K]_o$-related effects during ischemia stem from a $[K]_o$ elevation of resting membrane potential, $V_{rest}$. We investigated how changes in $[K]_o$ during simulated ischemia affect $V_{rest}$. In Fig. 3, $V_{rest}$ (solid line, as computed by the LRd model) and potassium reversal potential, $E_k$ (dotted line), are plotted against $[K]_o$. $E_k$ was computed by the Nernst equation at a temperature of 37°C and $[K]_i = 144.86$ mM (parameters of the LRd model). It can be observed that $V_{rest}$ closely
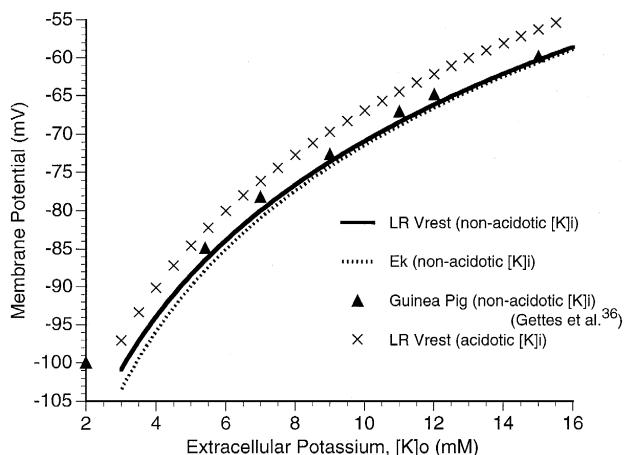


Fig. 3. Resting membrane potential, $V_{rest}$, vs. $[K]_o$ for non-acidic and acidic conditions. Solid line and x-symbol line show resting membrane potential, $V_{rest}$, of LRd model as $[K]_o$ is varied under non-acidic ($[K]_i = 144.8$ mM) and acidic ($[K]_i = 125$ mM) conditions, respectively. Dashed line is computed potassium Nernst potential, $E_K$ (non-acidic conditions). Triangles are measured resting membrane potential values for different values of $[K]_o$ from healthy guinea-pig ventricle muscle by Gettes et al. [36]. $V_{rest}$ is slightly more positive than $E_k$ at the lower range of $[K]_o$. As $[K]_o$ increases, $V_{rest}$ follows and approaches $E_k$. $[K]_o$ and $[K]_i$ are the extracellular and intracellular potassium concentrations.

follows $E_k$, reflecting the large resting membrane permeability to potassium through $I_{K1}$. $V_{rest}$ is less negative than $E_k$ at $[K]_o \leq 6.5$ mM, due to inward current from the sodium and calcium background currents, $I_{Na,b}$ and $I_{Ca,b}$, and the sodium–calcium exchanger, $I_{NaCa}$ (at control $[K]_o$ $E_k$ is 1.6 mV more negative than $V_{rest}$ which is slightly less but on the same order of 4 mV difference reported by Kléber [18] for guinea-pig heart). Increased $I_{K1}$ channel conductance at higher $[K]_o$ and decreased driving force of the inward currents diminish the deviation of $V_{rest}$ from $E_k$, and for $[K]_o > 6.5$ mM $V_{rest}$ is within 1 mV of $E_k$. Experimental recordings of $V_{rest}$ versus $[K]_o$ from guinea-pig ventricle [36] have been reproduced in Fig. 3 (filled triangles). The simulation closely approximates recorded $V_{rest}$ as $[K]_o$ is varied.

Ischemic $V_{rest}$ is affected by conditions of acidosis, in addition to the condition of increased $[K]_o$. Acidosis reduces $[K]_i$ which, from Fig. 3 (x symbols), depolarizes $V_{rest}$ about 3.8 mV (3.7 mV depolarization at $[K]_o = 3$ mM and 4.0 mV depolarization at $[K]_o = 16.0$ mM). The other effects of acidosis ($I_{Na}$ and $I_{Ca(L)}$ changes) and all effects of anoxia ($I_{K(ATP)}$) have minimal effect on $V_{rest}$.

### 3.2. Action potential upstroke

In Fig. 4 we investigate the effect of $V_{rest}$ depolarization on the action potential upstroke parameters. The figure contains peak upstroke velocity ($(dV_m/dt)_{max}$, solid line), maximum sodium current (long dashed line, mostly obscured by $(dV_m/dt)_{max}$), and resting sodium channel availability ($(h \cdot j)_{rest}$, short dashed line) versus resting potential. $h$ and $j$ are the fast and slow inactivation gates of $I_{Na}$, respectively [4,37]. Their product provides the fraction of available sodium channels. $[K]_o$ values corresponding to the resting potential are also shown on the abscissa. Moderate increases in $[K]_o$ to $[K]_o < 6$ mM cause a slight increase in $(dV_m/dt)_{max}$ due to reduced depolarization time to threshold without resting sodium channel inactivation. Further $[K]_o$ elevation, up to $[K]_o = 15$ mM, causes a decrease in resting sodium channel availability which reduces peak $I_{Na}$ and $(dV_m/dt)_{max}$. In this range of $[K]_o$ $(dV_m/dt)_{max}$ is coincident with $I_{Na,max}$, i.e., the action potential upstroke is supported by $I_{Na}$. In regions of $[K]_o > 15$ mM an interesting phenomenon occurs, $(dV_m/dt)_{max}$ becomes independent of $I_{Na,max}$. At $[K]_o = 15$ mM, the action potential upstroke is 'taken over' by calcium current. That is, $I_{Ca(L),max}$ (not shown) is greater than $I_{Na,max}$ (for $[K]_o = 17$ mM, $I_{Ca(L),max}$ is 15.5 $\mu$A/$\mu$F and $I_{Na,max}$ is 5.4 $\mu$A/$\mu$F). At all values of $[K]_o > 15$ mM, $(dV_m/dt)_{max}$ is coincident with $I_{Ca(L),max}$. Calcium takeover at $[K]_o = 15$ mM is highlighted in the inset of Fig. 4.

Because acidosis reduces sodium channel and calcium channel conductances, it should affect the calcium takeover potentials and the viability of the upstroke. The effects of combined acidosis and elevated $[K]_o$ on $(dV_m/dt)_{max}$ are
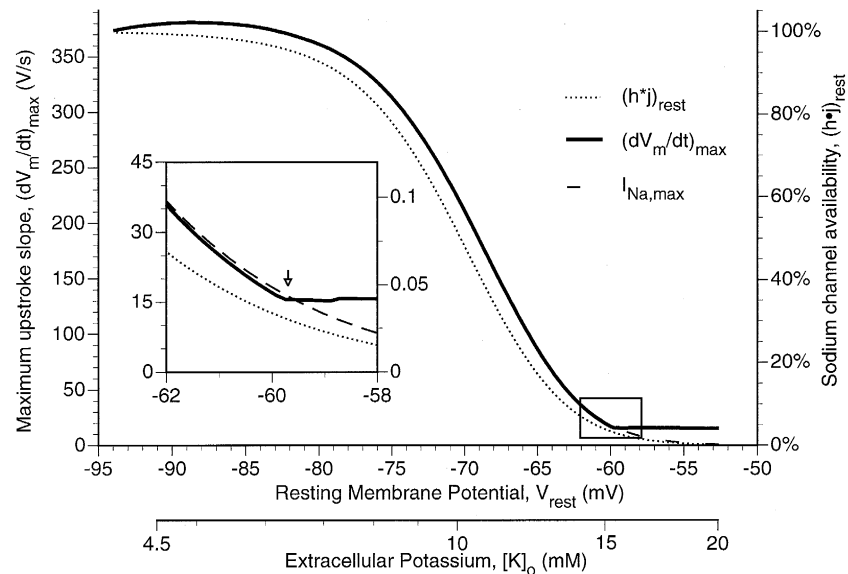
Fig. 4. Upstroke dependence on resting potential. Maximum upstroke velocity $(dV_m/dt)_{max}$ (thick solid line), sodium channel availability $(h \cdot j)_{rest}$ (short dashed line), and maximum sodium current during the upstroke, $I_{Na,max}$ (long dashed line), for different resting potentials altered by raising extracellular potassium $[K]_o$. $(dV_m/dt)_{max}$ is dominated by $I_{Na}$ until $V_m \sim -60$ mV at which $(h \cdot j)_{rest}$ is 3%. This is the point of $I_{Ca(L)}$ takeover.

shown in Fig. 5. The two large curves correspond to a control cell subjected to elevated $[K]_o$ (curve 1) and an acidic cell subjected to elevated $[K]_o$ (curve 2). Stimulus strength in this simulation was reduced to $-50$ μA/μF to reflect suppressed source current from neighboring cells during acute ischemia in the (multicellular) myocardium. Two observations can be made from Fig. 5: acidic $(dV_m/dt)_{max}$ is less than control $(dV_m/dt)_{max}$ at any $[K]_o$, and calcium takeover does not occur in acidic cells. Acidic

$(dV_m/dt)_{max}$ is less than control $(dV_m/dt)_{max}$ because acidosis reduces $\bar{g}_{Na}$. Calcium takeover for the non-acidic cell occurred at $[K]_o = 15$ mM. Because $(dV_m/dt)_{max}$ is reduced ($I_{Na}$ is suppressed), takeover for the acidic cell would have occurred earlier, at $[K]_o = 12.5$ mM, if $I_{Ca(L)}$ were not affected by acidosis. However, calcium current under acidic conditions is compromised and is insufficient to sustain the upstroke. The result is excitation failure. This is further illustrated in Fig. 5 by showing the first 10
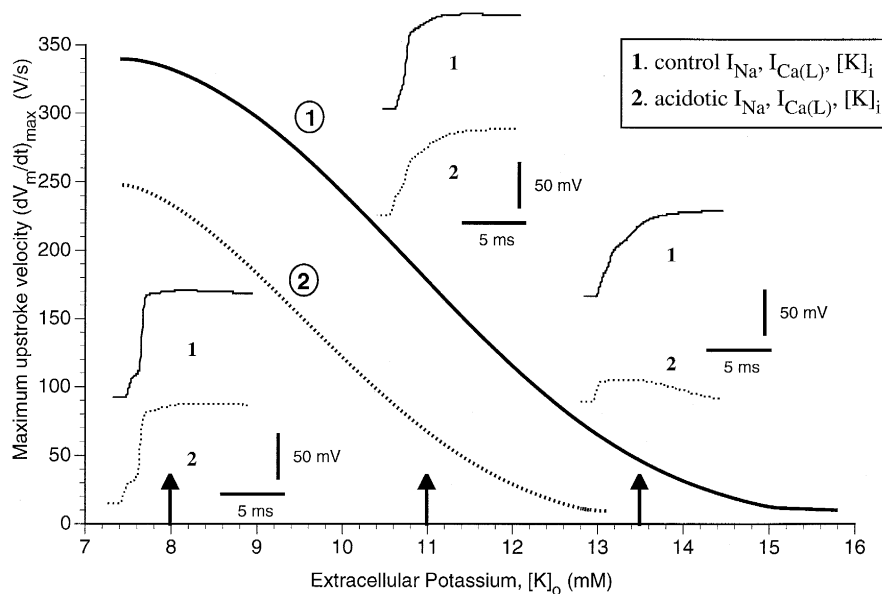


Fig. 5. Depression of maximum upstroke velocity as extracellular potassium is raised for control and acidic conditions. $(dV_m/dt)_{max}$ for control (solid line, curve 1) and acidic (dotted line, curve 2) conditions with increasing $[K]_o$. Acidosis causes a $[K]_o$ independent depression of $(dV_m/dt)_{max}$ and prevents calcium takeover which would otherwise occur at $[K]_o \sim 13$ mM. The first 10 ms of the control (1) and acidic (2) upstrokes are shown for $[K]_o = 8$ mM, 11 mM, 13.5 mM (insets). Stimulus current was reduced to $-50$ μA/μF to reflect decreased excitatory current during acute ischemia.
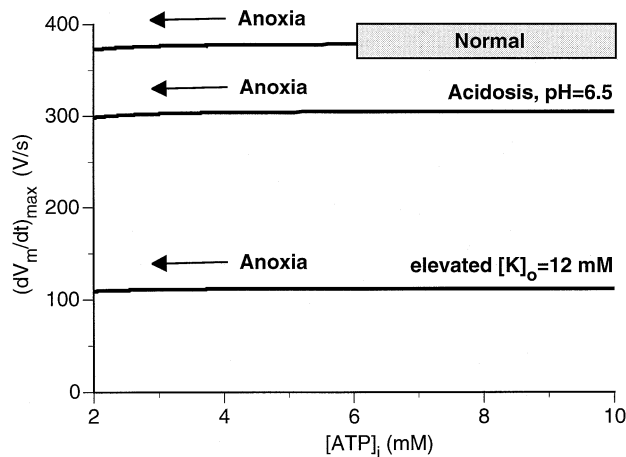
Fig. 6. Effect of anoxia on maximum upstroke velocity. $(dV_m/dt)_{max}$ computed as a function of $[ATP]_i$. Reduced $[ATP]_i$ causes opening of $I_{K(ATP)}$. The top, middle, and bottom curves correspond to conditions of (pH ~ 7.4, $[K]_o$ = 4.5 mM), (pH ~ 6.5, $[K]_o$ = 4.5 mM), and (pH ~ 7.4, $[K]_o$ = 12.0 mM), respectively. At the entire ischemic range of $[ATP]_i$, acidosis causes marginal reduction in $(dV_m/dt)_{max}$ and elevated $[K]_o$ causes major reduction in $(dV_m/dt)_{max}$. For each condition, $[ATP]_i$ reduction has minor effect on $(dV_m/dt)_{max}$. 'Normal' indicates control, non-ischemic conditions.

ms of action potential upstrokes for $[K]_o$ = 8, 11 and 13.5 mM. At $[K]_o$ = 8 mM the upstrokes for the control (1) and acidic (2) action potentials are similar. At $[K]_o$ = 11 mM, acidic slowing of the upstroke (2) is readily apparent. At $[K]_o$ = 13.5 mM, sodium current brings the control cell (1) into the range of calcium activation and calcium current supports the latter half of the upstroke. In the acidic cell (2), the stimulus fails to evoke a sodium response and calcium current is unable to support further excitation, resulting in excitation failure and return to $V_{rest}$.

To determine the impact of anoxia on membrane excitability of the isolated cell, we computed $(dV_m/dt)_{max}$ for a full range of ischemic $[ATP]_i$ (2–10 mM) with and without the conditions of elevated $[K]_o$ and acidosis. Data are shown in Fig. 6. The top curve corresponds to simulations with anoxic conditions alone, via activation of $I_{K(ATP)}$. The middle curve corresponds to anoxic conditions together with acidosis (corresponding to pH = 6.5), and the bottom curve corresponds to anoxia with elevated $[K]_o$ ($[K]_o$ = 12 mM). The stimulus was constant at −80 $\mu A/\mu F$ for all simulations. It is apparent from the down shift of the $(dV_m/dt)_{max}$ curves that acidosis causes minor (19%) and elevated $[K]_o$ causes major (70%) depression of excitability. Anoxia has little effect on excitability. When $[ATP]_i$ is reduced from 10–2 mM, $(dV_m/dt)_{max}$ is reduced by only 1.6%, 2.3%, and 2.7% for the top, middle, and bottom curves, respectively. Fig. 6 illustrates that if anoxia depresses membrane excitability by activation of $I_{K(ATP)}$, it does so at $[ATP]_i$ below the ischemic range.

### 3.3. Action potential duration (APD)

Ischemic shortening of action potential duration is the result of increased net outward current during the plateau, reflecting some combination of increased outward current and decreased inward currents. Elevated $[K]_o$ increases outward current by a direct effect on the $[K]_o$ dependent potassium currents, $I_{K1}$ and $I_{Kr}$. Also, outward current is enhanced by the anoxic decrease in available $[ATP]_i$, which opens the normally dormant $I_{K(ATP)}$. Inward current reduction is the result of both acidic and anoxic reduction of $I_{Ca(L)}$. We evaluated the quantitative influence of these three processes on APD. Results are shown in Fig. 7. Panels A, B and C contain APD versus $[K]_o$, $[ATP]_i$ and $\bar{I}_{Ca(L)}$, respectively. The gray zone in each panel corresponds to the range of values assumed by each parameter
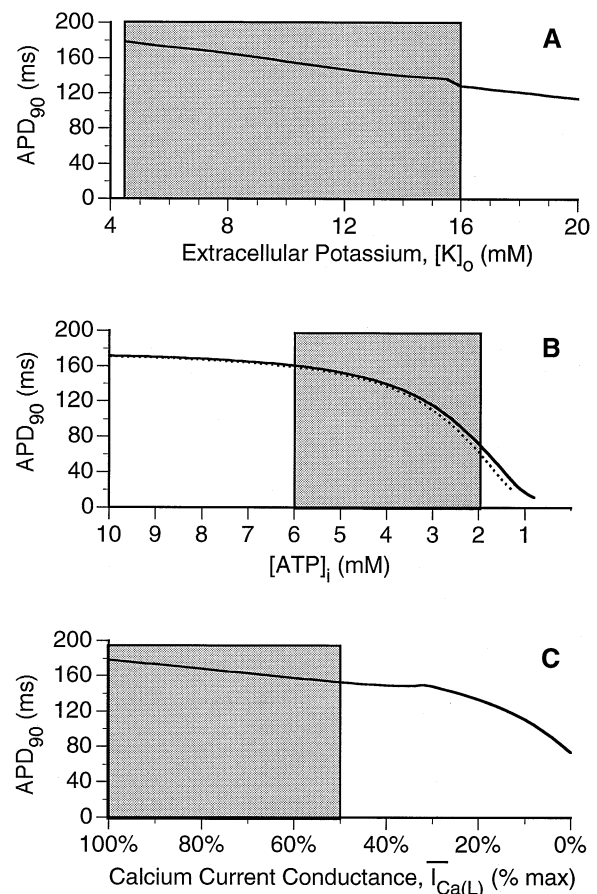


Fig. 7. Changes in action potential duration for the three major component conditions of acute ischemia. (A) *Hyperkalemia*. Action potential duration computed from time of $(dV_m/dt)_{max}$ to 90% repolarization ($APD_{90}$) versus extracellular potassium concentration. (B) *Anoxia*. $APD_{90}$ versus $[ATP]_i$. $[ATP]_i$ reduction due to anoxia increases the conductance of the ATP-dependent potassium channel, $I_{K(ATP)}$, and decreases conductance of $I_{Ca(L)}$. Solid line corresponds to anoxic regulation of $I_{K(ATP)}$ alone and dotted line corresponds to anoxic regulation of both $I_{K(ATP)}$ and $I_{Ca(L)}$. (C) *Acidosis*. $APD_{90}$ versus maximum conductance of the L-type calcium current, $\bar{I}_{Ca(L)}$. The conductance is decreased by intracellular acidosis. The shaded regions in each panel correspond to the range of values during acute ischemia.

during acute ischemia. In Panel A, elevated $[K]_o$ contributes to APD shortening in a linear fashion proportional to $[K]_o$. However its contribution is small, causing a 20 ms reduction of APD at $[K]_o = 12$ mM. Similarly, acidosis-related reductions in $\bar{I}_{Ca(L)}$ reduce APD (Panel C) in a linear fashion, causing 20 ms APD reduction at 50% $\bar{I}_{Ca(L)}$ reduction. Further reductions of $\bar{I}_{Ca(L)}$ to about 20–30% of maximum cause significant reduction of APD, but it is unlikely that $\bar{I}_{Ca(L)}$ is reduced to this degree during acute ischemia. $[ATP]_i$ reductions, within the ischemic range, have a marked effect on APD (Panel B). The solid and dotted lines in Panel B correspond to effects of $[ATP]_i$ on $I_{K(ATP)}$ alone and on both $I_{K(ATP)}$ and $I_{Ca(L)}$, respectively. Comparison of the two lines indicates that the predominant effect of $[ATP]_i$ on APD is due to $I_{K(ATP)}$. Furthermore, at $[ATP]_i = 7$ mM, APD shortening is the same as that obtained from 25% acidic reduction of $\bar{I}_{Ca(L)}$ (i.e., 75% in Fig. 7C). At $[ATP]_i = 4.5$ mM, APD shortening is the same as from $[K]_o$ elevation to 12 mM. The steepness of the $I_{K(ATP)}$ Hill coefficient (indicating cooperative binding, Fig. 2A) causes a rapid decline of APD at $[ATP]_i < 4.5$ mM. At $[ATP]_i = 2$ mM, the lower end of feasible ATP concentration during acute ischemia, APD is reduced to 72 ms.

The APD relationships in Fig. 7 suggest that $I_{K(ATP)}$ is the dominant cause of ischemic APD shortening. In Fig. 8, we further explore not only the degree of shortening but also action potential shape changes under ischemic conditions. Fig. 8A contains the action potentials recorded by Friedrich et al. [11] of isolated guinea-pig cells subjected to complete anoxia. Data are shown at 0, 3, 6 and 9 min from the onset of APD shortening. Simulated action potentials that correspond to the ischemic range of $\%\bar{I}_{Ca(L)}$ and $I_{K(ATP)}$, i.e., the gray zones of Fig. 7, are shown in Fig. 8B (solid lines) and Fig. 8C, respectively. It can be immediately observed that ischemic reductions of $\bar{I}_{Ca(L)}$ fail to cause significant APD reduction (Fig. 8B). The dashed curve in Fig. 8B corresponds to an action potential at 0% $\bar{I}_{Ca(L)}$, illustrating that decreased $\bar{I}_{Ca(L)}$ can cause major APD reduction, but at levels well beyond the ischemic range. Furthermore, the characteristics of APD shortening in the experimental data (Fig. 8A) are similar to those computed during $I_{K(ATP)}$ induced shortening (Fig. 8C). It is very different from the behavior during decreased-$\bar{I}_{Ca(L)}$ induced shortening. Action potential amplitude decreases in the Friedrich data (Fig. 8A) and in the $I_{K(ATP)}$-influenced action potential (Fig. 8C), but not in the $\bar{I}_{Ca(L)}$-influenced action potentials (Fig. 8B). Due to its driving force, $I_{K(ATP)}$ is largest at peak $V_m$, at the start of the plateau. Thus $I_{K(ATP)}$ exerts its major effect early in the plateau which accelerates early repolarization. In contrast, both $I_{Ca(L)}$ driving force and recovery from inactivation increase with repolarization from peak $V_m$. This explains the late plateau and phase-III effects of reduced $\bar{I}_{Ca(L)}$ (Fig. 8B). Note that during most of the plateau, action potentials for different degrees of $\bar{I}_{Ca(L)}$ suppression overlap with no
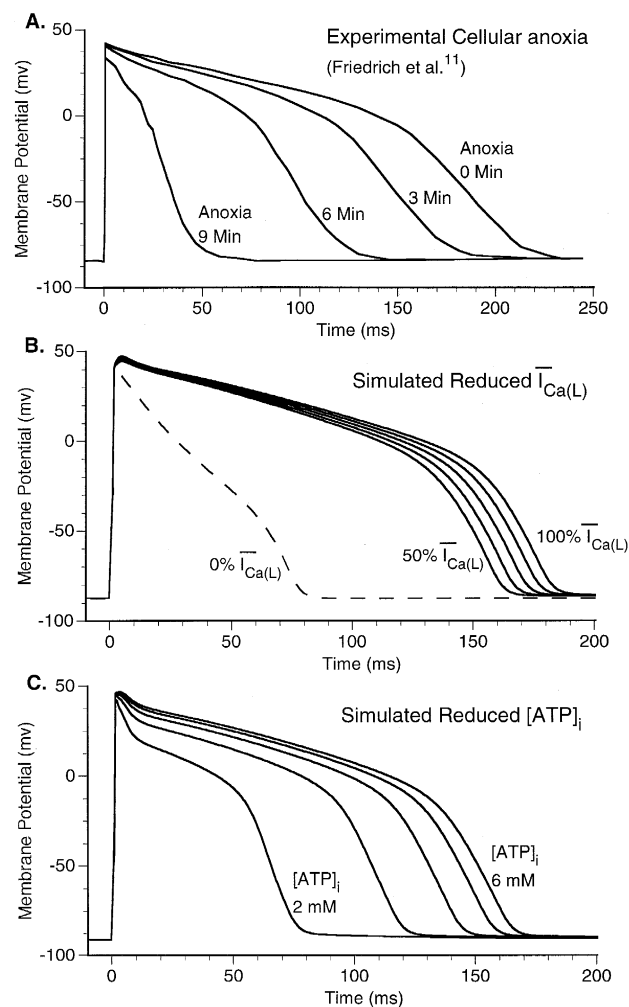


Fig. 8. Comparison of action potential shape changes between experimental anoxic conditions, simulated reduction in $I_{Ca(L)}$ and simulated effect of $I_{K(ATP)}$ at different $[ATP]_i$. (A) Action potentials recorded by Friedrich et al. [11] of isolated guinea-pig ventricular cells under conditions of anoxia. 0 min corresponds to the time of first action potential shortening. (B) Action potentials computed after decreasing maximum $I_{Ca(L)}$ conductance within the range that occurs during acute ischemia (0–50% decrease). The extreme case of complete $I_{Ca(L)}$ block, which is outside the range of ischemic conditions, is shown for reference (dashed curve). (C) Action potentials computed after decreasing $[ATP]_i$ from 6 mM to 2 mM (in steps of 1 mM), the range of values likely to occur during acute ischemia.

apparent amplitude changes. Differentiation of these action potentials occurs only very late. The inconsistency with the experimental observation of the simulated $\bar{I}_{Ca(L)}$-dependent shape changes and degree of APD reduction indicates that this current can not be responsible for ischemic action potential shortening. The fact that $I_{K(ATP)}$ alone can reproduce these changes faithfully (Figs. 7 and 8), strongly indicates that $I_{K(ATP)}$ is the major mechanism of ischemic APD shortening.

### 3.4. Recovery of excitability

Cardiac membrane normally recovers excitability on the tail of a preceding action potential. Full excitability begins with the return to resting potential. Elevated $[K]_o$ and other conditions of ischemia delay the recovery of excitability beyond the return to $V_{rest}$, a phenomenon known as 'post-repolarization refractoriness'. In Fig. 9, we investigate the delay in recovery of excitability caused by elevated $[K]_o$. In each set of simulations a conditioning action potential is initiated at time $= 0$ by stimulus S1 and secondary action potentials are obtained with a second stimulus S2 at increasing diastolic intervals (DI, time between 95% repolarization of the first action potential and the start of S2). Panels A and B correspond to control conditions ($[K]_o = 4.5$ mM) and Panels C and D correspond to conditions of elevated potassium ($[K]_o = 12$ mM). Under control conditions the first successful S2 action potential occurs at $S1 - S2 = 181$ ms (DI $= -1.8$ ms, which corresponds to 93% repolarization of the first action potential). Beyond 181 ms, $(dV_m/dt)_{max}$, a measure of membrane excitability, is restored rapidly in a monoexponential fashion with a time constant of $\tau = 10.3$ ms (Panel B). Therefore $(dV_m/dt)_{max}$ is 44% recovered at DI $= 10$ ms and 89% recovered at DI $= 20$ ms. In Panel 9B we show the product of the two sodium channel inactivation gates $(h \cdot j)$ immediately prior to the S2 stimulus (this product provides the degree of $I_{Na}$ recovery and the fraction of available sodium channels). $(h \cdot j)_{S2}$ recovered with a time constant $\tau = 12.5$ ms, similar to the time constant of $(dV_m/dt)_{max}$ recovery, indicating that recovery of excitability is achieved by recovery from sodium channel inactivation. Time constants of the sodium channel inactivation gates depend on the membrane potential. Because $[K]_o$ determines resting membrane potential, it is then expected that elevated $[K]_o$ will alter the time constant of $I_{Na}$ recovery. Panels 9C and 9D contain simulations run at $[K]_o = 12$ mM. The first successful S2 action potential for $[K]_o = 12$ mM occurred at $S1 - S2 = 171$ ms (DI $= 22$ ms). Thereafter $(dV_m/dt)_{max}$ recovery occurred with a time constant of 81.4 ms, close to the $(h \cdot j)_{S2}$ time constant of 88.8 ms (Panel 9D). Note the eight fold increase in $\tau$ of $(h \cdot j)_{S2}$ relative to control which is due to the change in $V_{rest}$ from $-91$ mV ($[K]_o = 4.5$ mM) to $-66$ mV ($[K]_o = 12$ mM).

Acidosis and anoxia affect the action potential shape and the sodium current, and therefore will modify recovery of excitability. In Fig. 10, the effect of these two conditions are evaluated when superimposed on control conditions (Panel A) and on elevated $[K]_o$ (Panel B). Each panel shows $(dV_m/dt)_{max}$ versus S1–S2 interval for the condition of $[K]_o$ alone, $[K]_o$ with acidosis, and $[K]_o$ with anoxia. A horizontal line is drawn at the bottom of each curve from the start of excitability to 95% repolarization of the previous action potential (DI $= 0$ ms, indicated by an
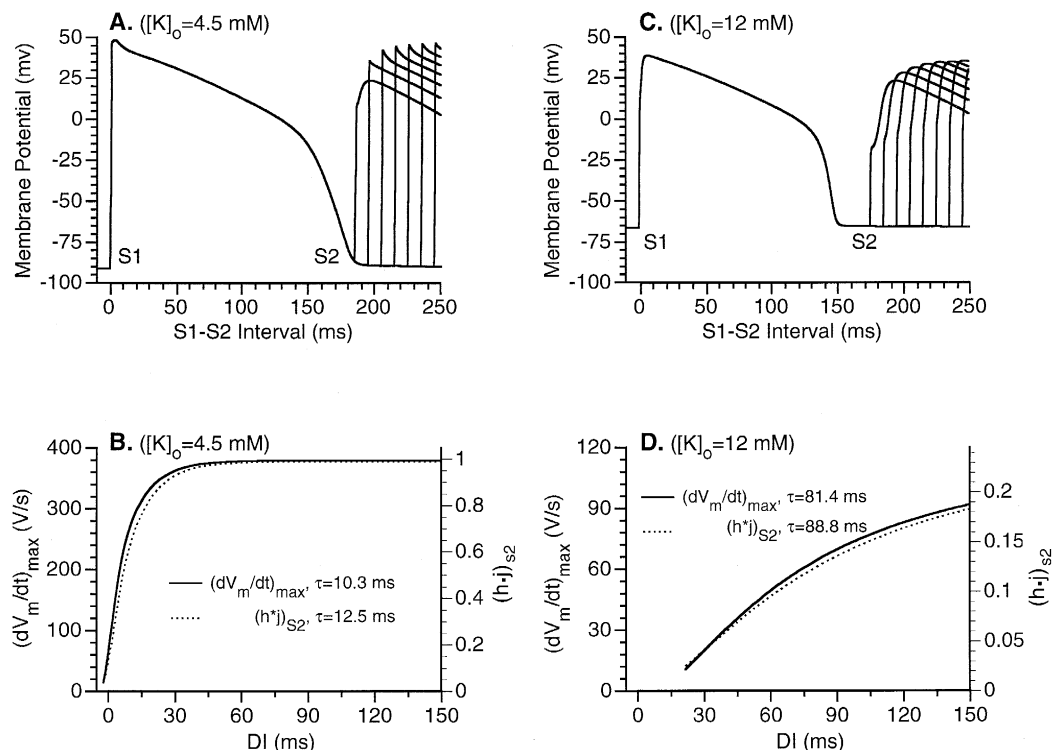


Fig. 9. Recovery of excitability under control conditions (left) and for elevated $[K]_o$ (right). (A) and (C) Action potentials obtained with a double (S1S2) pulse protocol where stimulus S1 initiates the conditioning action potential and S2 is the premature stimulus. (B) and (D) Recovery of $(dV_m/dt)_{max}$ (solid line) and sodium channel availability prior to the S2 stimulus $(h \cdot j)_{S2}$ (dotted line) computed from action potentials in (A) and (C), respectively. Diastolic interval (DI) of 0 corresponds to 95% repolarization of the conditioning action potential. (A) and (B) were computed at $[K]_o = 4.5$ mM and (C) and (D) were computed at $[K]_o = 12$ mM.
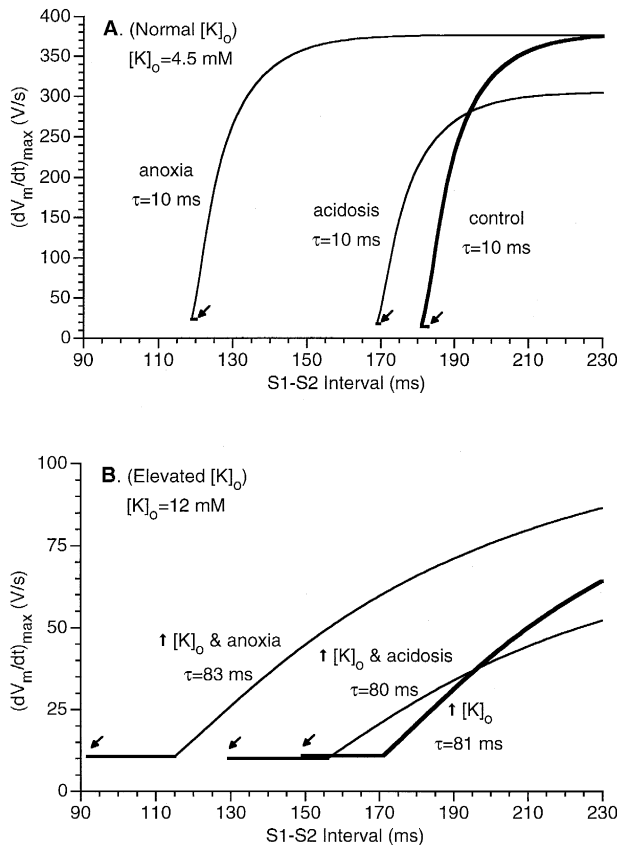
Fig. 10. Effect of acidosis and anoxia on recovery of excitability. Maximum upstroke velocity, $(dV_m/dt)_{max}$, for control, anoxic ($[ATP]_i = 3$ mM) and acidic (approximating pH $\sim 6.5$) conditions at normal $[K]_o = 4.5$ mM (A) and elevated $[K]_o = 12$ mM (B). Time constants of recovery of excitability, $\tau$, are shown for each curve. S1–S2 interval corresponds to protocol defined in Fig. 8. Note, in absolute terms, anoxia causes earlier onset of recovery relative to time of S1 due to APD shortening and acidosis decreases maximum $(dV_m/dt)_{max}$. However neither anoxia nor acidosis significantly affect the time course of recovery, $\tau$, with only minor effects on time to start of recovery from the end of the action potential. Horizontal lines at the beginning of each curve indicate time to start of recovery from 95% repolarization of the action potential (DI = 0, arrows).

### 3.5. Integrated ischemic model

To this point, we attempted to differentiate the electrophysiologic effects of the three major individual components of acute ischemia. Much of the difficulty in elucidating a cause and effect relationship between the metabolic and ionic conditions of ischemia and the ischemic electrical changes lies in the complicated interrelationships between events. For example, APD shortening can be due to acidotically reduced $I_{Ca(L)}$, and/or an enhanced outward $I_{K(ATP)}$ and/or elevated $[K]_o$. To combine the conditions, we selected individual parameter values that correspond to approximately the same time during the acute ischemic period. At 10 min of ischemia, tissue and cellular preparations retain a highly depressed but still viable electrical excitability during which $[K]_o$ is approximately 12 mM,
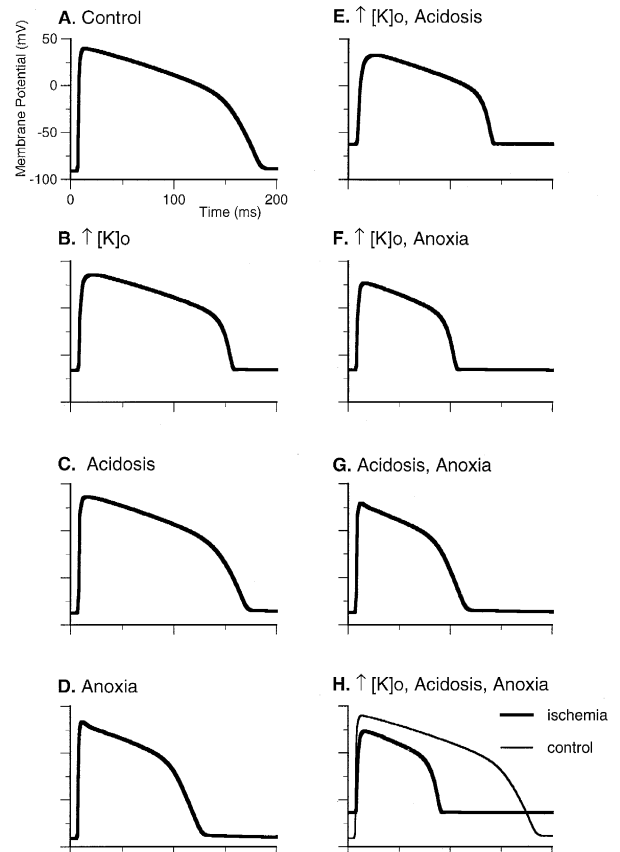


Fig. 11. Action potentials corresponding to different components of ischemia. Action potentials obtained from cell model corresponding to different combinations of the three components of ischemia: (A) control; (B) elevated $[K]_o$; (C) acidic effects on sodium channel, calcium channel and $[K]_i$; (D) influence of $I_{K(ATP)}$ at $[ATP]_i = 3$ mM; (E)–(H) combinations of elevated $[K]_o$, acidic and anoxic components. In (H) the fully integrated ischemic action potential (dark curve) and the control action potential (light curve) from (A) are superimposed for direct comparison. The abscissa and ordinate for all panels are adjusted to the scales indicated in (A). $I_{K(ATP)}$ is the ATP-dependent potassium current. $[K]_o$ and $[K]_i$ are the extracellular and intracellular concentrations of potassium.

arrow). Both anoxia and acidosis reduce APD (reflected in the shortened S1–S2 interval) and acidosis reduces $(dV_m/dt)_{max}$, yet at normal $[K]_o$ the shortest DI (start of excitability relative to DI = 0) is similar for all conditions ($-1.8$ ms, $-1$ ms and $-0.8$ ms for control, anoxic and acidic conditions, respectively). When $[K]_o$ is elevated to 12 mM, however, the shortest DIs are different (23.2, 28.0 and 30.1 ms for control, anoxic and acidic conditions, respectively). Thus both anoxia and acidosis delay the start of excitability, and acidosis has a slightly greater effect than anoxia. After the start of excitability, the time constants of recovery are the same for all conditions at normal $[K]_o$, and show small differences between conditions at elevated $[K]_o$. At $[K]_o = 4.5$ mM, $\tau$ was 10 ms for all conditions. At $[K]_o = 12$ mM, $\tau$ increased from 81 ms to 83 ms for anoxia and decreased to 80 ms for acidosis.

Table 1
Effect of elevated $[K]_o$, acidosis and anoxia on rest potential ($V_{rest}$), maximum upstroke velocity (($dV_m/dt)_{max}$), and action potential duration ($APD_{90}$)

| | $[K]_o$ | pH | $O_2$ | $V_{rest}$ (mV) | $(dV_m/dt)_{max}$ (V/s) | $APD_{90}$ (ms) |
|---|---|---|---|---|---|---|
| A | | *control* | | −91 | 379 | 173 |
| B | ↑ | | | −66 | 112 | 147 |
| C | | ↓ | | −87 | 306 | 160 |
| D | | | ↓ | −91 | 376 | 117 |
| E | ↑ | ↓ | | −62 | 38 | 131 |
| F | ↑ | | ↓ | −66 | 111 | 96 |
| G | | ↓ | ↓ | −87 | 303 | 105 |
| H | | *integrated ischemia* | | −62 | 36 | 85 |

Letters in left column indicate corresponding panels of Fig. 11.

the acidic pH is about 6.5 and anoxia reduces $[ATP]_i$ to 3.0 mM [1,2,38,39]. Assigning typical single values to represent these conditions does not reflect ischemic heterogeneity, but is useful to assess the relative roles of these three component conditions in ischemic electrophysiological changes. Fig. 11 contains action potentials resulting from the three different conditions of ischemia in isolation and in different combinations. Panel A is the control action potential and Panels B, C and D correspond to action potentials subject to $[K]_o = 12$ mM, pH = 6.5 and $[ATP]_i = 3$ mM, respectively. Panels E, F and G reflect the combined contributions of two ischemic conditions; elevated $[K]_o$ and acidosis, elevated $[K]_o$ and anoxia, and acidosis and anoxia, respectively. Panel H corresponds to the action potential in the presence of all three conditions of simulated ischemia. A plot of the control action potential from Panel A (light line) is provided in Panel H for direct comparison.

Inspection of Fig. 11 allows visual estimation of the influence of each ischemic component. It is evident that elevated $[K]_o$ contributes significantly to resting depolarization, causes reduction in upstroke velocity and slight APD shortening (Panels A and B). The isolated effect of acidosis is minimal (Panels A and C) and anoxia, in isolation, causes APD shortening (Panel A and D). When present with elevated $[K]_o$, acidosis magnifies the $[K]_o$-induced upstroke depression (Panels B and E). Acidosis has little additional effect on the upstroke or APD when present in conjunction with anoxia (Panels D and G). To generalize, elevated $[K]_o$ affects all characteristics of the ischemic action potential by depolarizing $V_{rest}$, depressing the upstroke and reducing APD. Acidosis depresses the upstroke, and anoxia, the third ischemic condition, reduces APD.

A quantitative summary of the visual data in Fig. 11 is provided in Table 1. The complete ischemic conditions (last row) depolarize normal $V_{rest}$ by 29 mV and reduce $(dV_m/dt)_{max}$ and $APD_{90}$ by 82% and 51%, respectively. These values are within the experimental range for is-

chemic depression of electrical activity, 10 min into the onset of perfusion block. From Table 1 it is clear that anoxia has little effect on the action potential upstroke. Anoxia reduced $(dV_m/dt)_{max}$ from 379 V/s to 376 V/s when applied in isolation, and reduced $(dV_m/dt)_{max}$ from 38 V/s to 36 V/s when applied in the presence of elevated $[K]_o$ and acidosis. Although both elevated $[K]_o$ and acidosis contribute to reductions in $(dV_m/dt)_{max}$, the effect of elevated $[K]_o$ is greater. Individually, $[K]_o$ and acidosis reduce $(dV_m/dt)_{max}$ by 70% and 20%, respectively, a ratio of 3.5:1. With respect to APD, elevated $[K]_o$ reduces APD from 173 ms to 147 ms, but APD reduction is dominated by anoxia and the associated $I_{K(ATP)}$. The ratio of anoxia induced APD shortening to elevated $[K]_o$ induced APD shortening is 2.2:1. Acidosis has little effect on APD.

Major ionic currents during an ischemic action potential are shown in Fig. 12, left panel. These data show ionic current behavior under conditions of acute ischemia and can be compared to the respective currents under control conditions (right panel). The fast sodium current $I_{Na}$ (Panel B) is significantly reduced (due to elevated $[K]_o$ and acidosis) and, consequently, $I_{Ca(L)}$ (Panel C) supports the last portion of the upstroke (at $V_m > 0$ mV). Note that $I_{Ca(L)}$ is increased during ischemic conditions in spite of acidic depression of the maximum channel conductance. This reflects an increased driving force during the lower plateau of the ischemic action potential. The inward rectifier potassium current, $I_{K1}$ (Panel D), is enhanced as a direct result of elevated $[K]_o$. Anoxia results in activation of $I_{K(ATP)}$ which contributes a repolarizing current during the entire action potential (Panel C). The fast component of the delayed rectifier current, $I_{Kr}$ (Panel E), is relatively unchanged due to a balance between reduced driving force (depolarized $E_K$ and reduced action potential amplitude) and direct enhancement from elevated $[K]_o$. Because the slow component of the delayed rectifier ($I_{Ks}$) is not directly enhanced by elevated $[K]_o$, reduction in driving force and slower activation at decreased plateau potentials
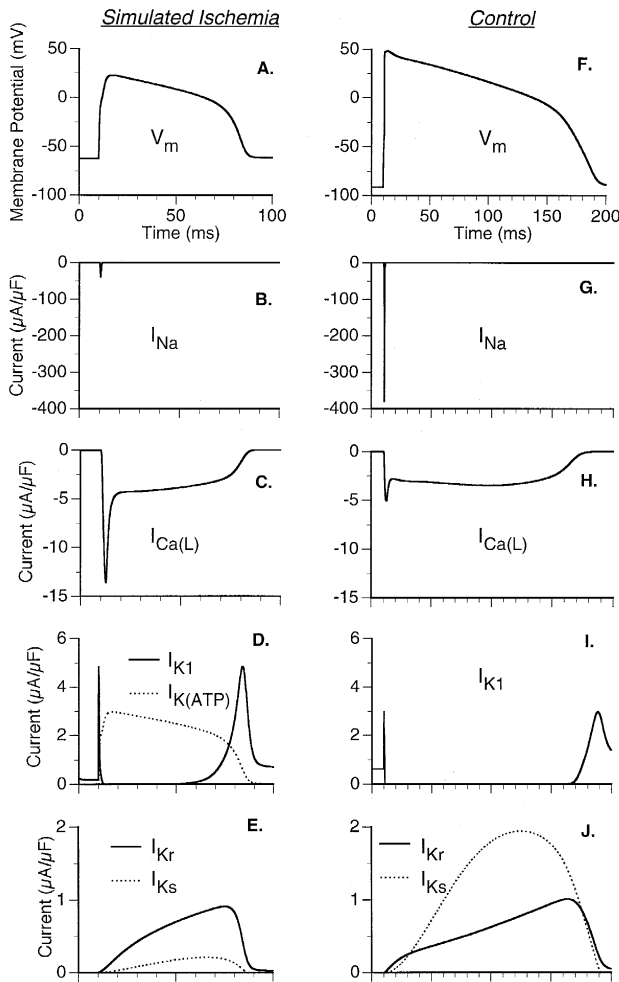
Fig. 12. Major ionic currents during an ischemic action potential. An ischemic action potential (A) and the principal ionic currents are shown for conditions of $[K]_o = 12$ mM, pH = 6.5, and $[ATP]_i = 3$ mM. The fast sodium and slow L-type calcium currents are in (B) and (C), the inward rectifier and ATP-dependent potassium currents are in (D), and the fast and slow components of the delayed rectifier potassium current are in (E). A control, non-ischemic action potential and corresponding currents are shown in (F)–(J) for comparison. Current symbols are identified in Fig. 1.

significantly reduce $I_{Ks}$ during the ischemic action potential.

## 4. Discussion

The results suggest that the major electrical changes of acute myocardial ischemia can be reproduced by the conditions of elevated $[K]_o$, acidic changes of the fast sodium and L-type calcium currents, acidic reduction of $[K]_i$, anoxia induced activation of a time independent outward current ($I_{K(ATP)}$), and slight anoxic reduction of $I_{Ca(L)}$. These conditions of ischemia in a cell-model formulated from otherwise non-pathological conditions successfully produced: (a) $V_{rest}$ depolarization at elevated $[K]_o$, (b) $[K]_o$

depression of $(dV_m/dt)_{max}$ with additional depression from acidosis, (c) APD shortening similar to that of isolated anoxic cells, and (d) delayed recovery of excitability (post-repolarization refractoriness). The model was developed from mostly single channel and single cell recordings of individual processes. The similarity of the simulated electrical behavior to observed ischemic electrical activity supports the use of the model to investigate mechanisms of electrophysiological changes due to ischemic conditions. Mechanistic insights gained from the simulations and limitations of the study are discussed below.

### 4.1. Membrane excitability

This study, in part, focused on the transition from $I_{Na}$ to $I_{Ca(L)}$ dominated upstrokes in single cells ('space-clamped' conditions). Without the complications of intercellular coupling, the results suggest that unmodified calcium current can maintain the upstroke at $[K]_o$ values that are elevated within the range of acute ischemia. Calcium current dominates the upstroke when $I_{Ca(L),max} > I_{Na,max}$. Because $I_{Na,max}$ is normally $\sim 400$ $\mu A/\mu F$ and $I_{Ca(L),max}$ is normally $\sim 10$ $\mu A/\mu F$, $I_{Na}$ needs to be $\sim 97\%$ inactivated (essentially fully inactive) before $I_{Ca(L)}$ is required to support the rising phase. Therefore the transition from $I_{Na}$ to $I_{Ca(L)}$ dominance occurs only when $I_{Na}$ fails due to resting inactivation. Acidosis depresses $I_{Na}$ at any $[K]_o$, and therefore $I_{Ca(L)}$ is required at lower $[K]_o$ in the presence of acidosis for the upstroke to be maintained. Yet acidosis also depresses $I_{Ca(L)}$. The combination of depressed $I_{Ca(L)}$ and more negative $V_{rest}$ (lower $[K]_o$) decreases the likelihood that $I_{Ca(L)}$ can activate and sustain the upstroke when $I_{Na}$ fails. This is evident in Fig. 5 where the non-acidic transition to calcium upstrokes occurred at $[K]_o = 15$ mM. The acidic transition would have occurred at $[K]_o = 12.5$ but failed due to depressed $I_{Ca(L)}$. The result was action potential failure.

These findings support the major role of $I_{Na}$ in depressed upstrokes of acute ischemia at any $V_{rest}$ at which $I_{Na}$ is still viable. Early studies such as those by Cranefield [40] suggested a major role of the L-type calcium current because action potentials were found in isolated cardiac fibers superfused with elevated $[K]_o$ and catecholamines (calcium current agonists). Ischemic cardiac regions have elevated $[K]_o$ and high norepinephrine levels due to sympathetic nerve catecholemine release following coronary occlusion. Thus during ischemia, conditions exist that would facilitate $I_{Ca(L)}$. However more recent evidence suggests that depressed upstrokes are supported by depressed sodium current. In vascularized hamster cardiac transplants, Gilmour and Zipes [41] could suppress depressed action potentials with the sodium channel blocker tetrodotoxin, but not with the calcium channel blocker verapamil. Kléber et al. [7] found that ischemic porcine ventricular cells become unresponsive at average $V_{rest} \geq -60.3$ mV, slow response action potentials only began to

appear at $V_{rest} \geq -48.5$ mV. Lidocaine depressed or abolished action potentials in the ischemic regions of isolated porcine hearts [42], suggesting a primary dependence on inward sodium current.

In this study we have shown that at $[K]_o$ values within the ischemic range, a transition potentially exists from $I_{Na}$ to $I_{Ca(L)}$ upstrokes. The transition occurs at the point of $I_{Na}$ failure, and is less likely in the presence of acidosis. These results were obtained in a single, 'space-clamped' cell in the absence of intercellular coupling and electrical loading. In a multicellular ischemic preparation it may be expected that the depolarizing source current is not as strong as the direct stimulus used in this study. In addition, loading by surrounding cells will reduce availability of local inward current for depolarization. For these reasons we expect that $I_{Ca(L)}$-dominated upstrokes in depressed membranes are even less likely to occur in a multicellular environment during acute ischemia. Future studies will be directed at determining the effects of source and sink currents from surrounding cells on properties of ischemic membranes.

A result that may counter conventional wisdom is that activation of $I_{K(ATP)}$ within the ischemic range of $[ATP]_i$ (2–10 mM), although having a major effect on action potential duration, does not affect membrane excitability (Fig. 6). The reason that outward $I_{K(ATP)}$ does not significantly counteract inward $I_{Na}$ during the upstroke is based on the difference in reversal potential between $I_{Na}$ and $I_{K(ATP)}$. Subthreshold depolarization occurs relatively close to resting potential which is very close to potassium reversal potential and very far from sodium reversal potential. In the extreme case that membrane conductances of $I_{Na}$ and $I_{K(ATP)}$ are identical (an exaggeration of ischemic $I_{K(ATP)}$), during subthreshold depolarization, the sodium current will still be much greater than that of the potassium current. At $V_m = -60$ mV, for example, the $I_{Na}:I_{K(ATP)}$ ratio of transmembrane driving forces is 4:1.

In the simulations we determined membrane excitability for the isolated cell by applying a brief strong stimulus, usually $-80$ $\mu A/\mu F$ for 0.5 ms. In multicellular tissue, cells are excited by weaker, greater duration electrotonic current supplied from adjoining excited cells. $I_{K(ATP)}$, by reducing plateau amplitude and duration of excited cells, can decrease voltage gradients between excited and unexcited cells, decreasing the electrotonic source current. We have shown [17] that activation of $I_{K(ATP)}$ at $[ATP]_i$ levels that are within the ischemic range can cause propagation failure when $I_{Na}$ is reduced. The results presented here support the principle that ischemic $I_{K(ATP)}$ exerts its effect by reduction of the electrotonic source current, *not* by direct reduction of membrane excitability.

### 4.2. Action potential duration

There is a general consensus, though not universal, that $I_{K(ATP)}$ is the major current responsible for action potential

duration shortening during acute ischemia [11,19,33]. Reservations about the role of $I_{K(ATP)}$ during acute ischemia are based on the $K_d$ (half maximal saturation) of this current that is in the micromolar (25–500 $\mu M$) [26,32,43] range whereas $[ATP]_i$ remains in the millimolar range ($\sim$ 2–5 mM) [44,45] during the ischemic period. Also, sulfonylureas that are used in studies to block $I_{K(ATP)}$ may affect cell metabolism [19,46], causing secondary changes in APD that are inadvertently attributed to $I_{K(ATP)}$ [39].

Our results provide three reasons for supporting $I_{K(ATP)}$ as the dominant factor in ischemic APD shortening. (1) Process of elimination. Elevation of $[K]_o$ and anoxic and acidic reduction of $I_{Ca(L)}$ to values within the range of acute ischemia do not cause significant APD shortening (Fig. 7). Our model did not suggest, and we are not aware of, other means of APD shortening (in a single cell). $I_{K(ATP)}$ alone can cause 50% (86 ms) APD shortening at $[ATP]_i = 2.25$ mM. At $[ATP]_i = 3$ mM, $I_{K(ATP)}$ caused a 56 ms reduction in APD whereas similar extreme values of acidosis and elevated $[K]_o$ caused only 13 ms and 31 ms shortening, respectively (Table 1). (2) $I_{K(ATP)}$ has a pronounced role in APD shortening even though its formulated conductance in the model is very conservative. Channel density, and hence maximum conductance, was taken from whole cell measurements which are approximately one third of the density estimate from single patch data (see Section 2). Even with this conservative formulation, the computed 50% APD shortening at $[ATP]_i = 2.25$ mM corresponds to only 1.2% activation of $I_{K(ATP)}$ (comparing favorably to experimental estimates of 0.7–1% $I_{K(ATP)}$ activation required for 50% APD shortening [28,47]). (3) Only $I_{K(ATP)}$ can cause shape changes in the computed action potential that are similar to the shape changes observed in anoxic guinea-pig cells. $I_{Ca(L)}$ reductions cause changes late in the action potential plateau whereas $I_{K(ATP)}$ causes changes early in the plateau similar to those measured in anoxic cells (Fig. 8).

Yan et al. [39] demonstrated in rabbit papillary muscle that APD shortening during acute no-flow ischemic conditions could be disassociated from cellular [ATP] levels, and that $[K]_o$ accumulation combined with hypoxia can be responsible for APD shortening without involvement of $I_{K(ATP)}$. $[K]_o$ increases alone did not, in our cellular model, cause significant APD shortening despite inclusion of $[K]_o$ dependent channels ($I_{K1}$, $I_{Kr}$, $I_{K(ATP)}$) and appropriate upstroke changes at different $[K]_o$. It is possible that hypoxia in the elevated $[K]_o$/hypoxia preparation [39] caused intracellular acidic changes which included $V_{rest}$ depolarization and $I_{Ca(L)}$ inhibition. With combined elevated $[K]_o$ and acidosis, APD is reduced by 24% (Table 1). Therefore although only $I_{K(ATP)}$ can cause major ($> 50\%$) APD shortening, the combined effect of acidosis and elevated $[K]_o$ remains quantitatively significant.

An effect of acidosis not incorporated into the simulations is inhibition of the sodium–calcium exchange cur-

rent, $I_{NaCa}$, by intracellular protons. Cytoplasmic acidosis of pH = 6.5 causes a 3–5 fold inhibition of $I_{NaCa}$ from control conditions, and $I_{NaCa}$ is almost completely inhibited at pH = 6.0 [48,49]. We found (simulation data not shown) that specific $I_{NaCa}$ block of a non-paced cell increased APD of a single action potential by only 3%. However, we caution that the effect of $I_{NaCa}$ on APD will vary significantly based on experimental conditions and protocol. For instance, lengthening of APD in this example is a result of decreased $I_{NaCa}$ transport of calcium into the cell during the action potential upstroke and consequent reduction of SR calcium release and of calcium-dependent inactivation of $I_{Ca(L)}$. If, when $I_{NaCa}$ is blocked, calcium release from the SR is kept identical to that when $I_{NaCa}$ is not blocked, APD decreases by 4%. In another example, if $I_{NaCa}$ is altered by exchange of 50% of the extracellular sodium ions with lithium ions during the early plateau of an action potential, APD decreases by 20% [50] (a result duplicated by our model simulation). The APD decreases significantly with this intervention since $I_{NaCa}$ remains outward (rather than becoming inward) during the late plateau phase of the action potential. These examples suggest that the effect of acidotic $I_{NaCa}$ on APD is marginal. They also illustrate that the $I_{NaCa}$ effects must be carefully considered in context of the specific protocol and in relation to other currents, especially that of $I_{Ca(L)}$ and its calcium-dependent inactivation.

### 4.3. Postrepolarization refractoriness

In vivo cardiac cells, whether or not ischemic, are subject to repetitive firing. Under normal conditions cell refractoriness is a function of $I_{Na}$ availability and extends little beyond the recovery of resting potential. During acute ischemia the refractory (absolute and relative) period prolongs despite continued shortening of the APD and may outlast full repolarization by hundreds of milliseconds. Kodama et al. [14] reported an increase in the time constant of $(dV_m/dt)_{max}$ recovery in guniea-pig papillary muscle from $\tau = 18.2$ ms at $[K]_o = 5$ mM to $\tau = 74.6$ ms at $[K]_o = 12$ mM. Our simulations computed similar changes in $\tau$, ranging from $\tau = 10.3$ ms at $[K]_o = 4.5$ mM to $\tau = 81.4$ ms at $[K]_o = 12$ mM (Fig. 9). We found the mechanism of delayed recovery of excitability to be almost exclusively due to the voltage-dependence of the recovery kinetics of the sodium channel inactivation gates, $h$ and $j$. $V_{rest}$ depolarization by elevated $[K]_o$ slows the recovery of $h$ and $j$ following an action potential. A stimulus prior to complete $h$ and $j$ recovery encounters a lower $(h \cdot j)_{rest}$ than under steady-state conditions which results in reduced sodium channel availability and reduced excitability.

In addition to the effect of elevated $[K]_o$ on $\tau$, Kodama et al. [14] found that hypoxia in combination with elevated $[K]_o$ causes greater prolongation of recovery. For example, at $[K]_o = 12$ mM, 15 min of hypoxia increased $\tau$ from 75 ms to 134 ms [14]. In contrast, Sano et al. [51] did not find

in dog ventricle significant hypoxia-induced prolongation of $\tau$. Consistent with Sano et al. [51], we found that anoxia did not significantly prolong $\tau$ at any $[K]_o$. With the addition of anoxic conditions, computed $\tau$ at $[K]_o = 12$ mM increased only 2% from 81 to 83 ms (Fig. 10).

We suggest that regional inhomogeneities of $[K]_o$ may have been present in the Kodama et al. [14] preparation to explain their observation of a synergistic effect of hypoxia and elevated $[K]_o$ on postrepolarization refractoriness. In superfused preparations, such as those of Kodama et al. [14], intramuscle $[K]_o$ and $CO_2$ may increase to values larger than that recorded at the muscle surface [52]. Under conditions of elevated $[K]_o$ and hypoxia, intramuscle cells could experience sufficient $[K]_o$ elevation to become inexcitable. Therefore cells closer to the perfusate will be subjected to constant load from intramuscle cells, and respond with delayed recovery of excitability. This suggests that hypoxia induced delay in recovery of excitability may be caused by electrotonic influences due to ischemic heterogeneity rather than by an intrinsic cellular mechanism.

The effect of acidosis on postrepolarization refractoriness, like that of anoxia, was marginal. Acidosis has two direct effects on the sodium current, it (1) reduces maximum conductance and (2) causes an apparent negative shift in observed membrane potential. Reduced maximum conductance lowers the maximum obtainable $(dV_m/dt)_{max}$, however it does not affect $I_{Na}$ activation and inactivation kinetics and therefore reduced conductance does not affect time course of recovery. The shift in membrane potential counters somewhat $[K]_o$-induced depolarization of resting potential. At $[K]_o = 12$ mM, the addition of acidosis reduced $\tau$ from 81 to 80.0 ms. This reduction, of 1.2%, is not significant relative to $[K]_o$-induced prolongation of $(dV_m/dt)_{max}$ recovery.

### 4.4. Additional ischemic conditions

The conditions of ischemia studied in our theoretical simulations are not an exhaustive representation of all ischemic conditions. There are several conditions we have elected not to include because either their effects require further experimental characterization or their presence is not relevant during the acute phase of ischemia. The accumulation of lipid metabolites such as palmitoylcarnitine and lysophosphatidylcholine may have direct inhibitory effects on $I_{Na}$ [53] and $I_{Ca(L)}$ [54]. When these conditions are further elucidated and quantified, they can be incorporated into theoretical models of ischemia.

The effect of acidosis on the cardiac potassium currents is unclear. An increase in the time dependent outward current ($I_K$) during intracellular acidosis has been reported [55], an effect oppostie to the observed [56] decrease in the time-independent outward current ($I_{K1}$) in the presence of intracellular and extracellular acidosis. The opposite effects of $I_K$ and $I_{K1}$ would have opposite effects on

APD. The net effect on APD may be very small [57] and requires further experimental investigation. In this study we have chosen to neglect any direct affect of acidosis on the $I_{Kr}$, $I_{Ks}$ and $I_{K1}$ potassium currents.

There is considerable evidence that pH-linked accumulation of $[Na]_i$ and $[Ca]_i$ is related to arrhythmias during reperfusion and reoxygenation [58]. However, during the acute phase of ischemia studied in this paper, intracellular Na and Ca accumulation is not significant to overall ischemic electrophysiology. A rise in $[Ca]_i$ under ischemic conditions is coincident with the secondary phase of $[K]_o$ rise, electrical inexcitability, rapid depletion of $[ATP]_i$ and irreversible cell damage (cell death) [59]. Recent data suggest that intracellular calcium may contribute to electrical abnormalities associated with acute ischemia [60]. However these data remain preliminary and the role of intracellular calcium requires further study.

The activation of $I_{K(ATP)}$ and its major effect on APD raise the possibility that modulation of other ATP-dependent electrogenic processes might influence the action potential during ischemia. In particular, the possibility of a suppressed sodium/potassium pump, $I_{NaK}$, should be evaluated. Typically, $[ATP]_i$ drops 40–60% [44] (to about 2.5 mM) during acute ischemia. Millimolar concentrations of ATP are adequate for supporting pump function and it has been shown that the pattern of $[K]_o$ rise and fall in acutely ischemic myocardium is consistent with a functioning Na/K pump [18]. This implies that during the acute phase, significant inhibition of the Na/K pump and a consequential change in $I_{NaK}$ do not occur and should not be included in the simulations. It is important to recognize that the high sensitivity of $I_{K(ATP)}$ to changes in $[ATP]_i$ is due to its extremely high channel-density (comparable to that of $I_{Na}$). In fact, at $[ATP]_i = 3.0$ mM $I_{K(ATP)}$ is only 0.8% activated yet, due to its large density, its effect on APD is very significant.

Finally, the direct effects of ischemia on certain membrane ionic currents (Fig. 1) might lead to major, indirect changes in other ionic currents during the action potential. An example is shown in Fig. 12, where $I_{Ks}$ is greatly reduced secondary to changes in the ischemic action potential (e.g., reduced amplitude). The large effect of ischemia on $I_{Ks}$, in the absence of direct modulation of this current (Fig. 1), serves as an example of the complexity of electrical changes under ischemic conditions. Such indirect changes should be carefully considered in the interpretation of experimental observations and in the identification of targets for pharmacological management of ischemic arrhythmias.

## Acknowledgements

## Appendix A

Modeling ischemic conditions with the LRd model [4–6]: parameter values and formulation of $I_{K(ATP)}$.

*Elevated $[K]_o$*

$[K]_o$ varied between control (4.5 mM) and 16 mM, $[K]_o = 12.0$ mM for integrated ischemic model.

*Acidosis (pH = 6.5)*

$[K]_i = 125.0$ mM,
$V_{m,acid} = V_m - 3.4$ for all sodium current computations ($m$, $h$, $j$, $\tau_m$, $\tau_h$, $\tau_j$, and driving force),
$\bar{g}_{Na,acid} = 0.75 \cdot \bar{g}_{Na}$ for integrated ischemic model,
$\bar{g}_{Ca,acid} = 0.75 \cdot \bar{g}_{Ca}$ for integrated ischemic model.

*Anoxia-formulation of $I_{K(ATP)}$*

$I_{K(ATP)} = \bar{g}_{K(ATP)} \cdot (V_m - E_k)$,
$\bar{g}_{K(ATP)} = G_{K(ATP)} \cdot P_{ATP} \cdot ([K]_o/[K]_{o,normal})^n$,
$G_{K(ATP)} = 195 \cdot 10^{-6}/\text{Nichols}_{area}$ (nS/cm$^2$),

$$P_{ATP} = \frac{1}{1 + \left(\dfrac{[ATP]_i}{k_{0.5}}\right)^H}$$

$E_k$ = potassium reversal potential,
$\text{Nichols}_{area} = 5 \cdot 10^{-3}$ cm$^2$, Reference [28],
$[ATP]_i = 3.0$ mM for integrated ischemic model,
$[K]_{o,normal} = 4.0$ mM, $n = 0.24$, $H = 2$, $k_{0.5} = 0.250$ μM.

*Anoxia-formulation of $P_{Ca(L),(ATP)}$*

$$P_{Ca(L),ATP} = \frac{1}{1 + \left(\dfrac{k_{0.5}}{[ATP]_i}\right)^H}$$

$[ATP]_i = 3.0$ mM for integrated ischemic model,
$H = 2.6$, $k_{0.5} = 1.4$ mM.

## References

[1] Gettes LS, Cascio WE. Effect of acute ischemia on cardiac electrophysiology. In: Fozzard HA, Jennings RB, Haber E, Katz AM, Morgan HE, editors. The heart and cardiovascular system. New York: Raven Press, 1992:2021–2054.

[2] Wit AL, Janse MJ. The ventricular arrhythmias of ischemia and infarction: electrophysiological mechanisms. New York: Futura Publishing Company, 1992:648.

[3] Cascio WE, Johnson TA, Gettes LS. Electrophysiologic changes in ischemic ventricular myocardium: I. Influence of ionic, metabolic and energetic changes. J Cardiovasc Electrophys 1995;6:1039–1062.

[4] Luo CH, Rudy Y. A dynamic model of the cardiac ventricular action potential. I. Simulations of ionic currents and concentration changes. Circ Res 1994;74:1071–1096.

[5] Luo CH, Rudy Y. A dynamic model of the cardiac ventricular action potential. II. Afterdepolarizations, triggered activity, and potentiation. Circ Res 1994;74:1097–1113.

[6] Zeng J, Laurita KR, Rosenbaum DS, Rudy Y. Two components of the delayed rectifier $K^+$ current in ventricular myocytes of the guinea-pig type: theoretical formulation and their role in repolarization. Circ Res 1995;77:140–152.

[7] Kléber AG, Janse MJ, Wilms Schopmann FJ, Wilde AA, Coronel R. Changes in conduction velocity during acute ischemia in ventricular myocardium of the isolated porcine heart. Circulation 1986;73:189–198.

[8] Kléber AG, Janse MJ, Van Capelle FJ, Durrer D. Mechanism and time course of S-T and T-Q segment changes during acute regional myocardial ischemia in the pig heart determined by extracellular and intracellular recordings. Circ Res 1978;42:603–613.

[9] Arita M, Kiyosue T. Modification of 'depressed fast channel dependent slow conduction' by lidocaine and verapamil in the presence or absence of catecholamines-evidence for alteration of preferential ionic channels for slow conduction. Jpn Circ J 1983;47:68–81.

[10] Cranefield PF. The conduction of the cardiac impulse. Mount Kisco, NY: Futura Publishing, 1975:404.

[11] Friedrich M, Benndorf K, Schwalb M, Hirche H. Effects of anoxia on K and Ca currents in isolated guinea pig cardiocytes. Pflugers Arch 1990;416:207–209.

[12] Schütz E. Elektrophysiologie des Herzens bei einphasischer Ableitung. Ergebn Physiol 1936;38:493–620.

[13] Downar E, Janse MJ, Durrer D. The effect of acute coronary artery occlusion on subepicardial transmembrane potentials in the intact porcine heart. Circulation 1977;56:217–224.

[14] Kodama I, Wilde A, Janse MJ, Durrer D, Yamada K. Combined effects of hypoxia, hyperkalemia and acidosis on membrane action potential and excitability of guinea-pig ventricular muscle. J Mol Cell Cardiol 1984;16:247–259.

[15] Pogwizd SM, Corr PB. Reentrant and nonreentrant mechanisms contribute to arrhythmogenesis during early myocardial ischemia: results using three-dimensional mapping. Circ Res 1987;61:352–371.

[16] Kaplinsky E, Ogawa S, Balke CW, Dreifus LS. Two periods of early ventricular arrhythmia in the canine acute myocardial infarction model. Circulation 1979;60:397–403.

[17] Shaw RM, Rudy Y. Electrophysiologic effects of acute myocardial ischemia: a mechanistic investigation of action potential conduction and failure. Circ Res 1997;80:124–138.

[18] Kléber AG. Resting membrane potential, extracellular potassium activity, and intracellular sodium activity during acute global ischemia in isolated perfused guinea pig hearts. Circ Res 1983;52:442–450.

[19] Wilde AA, Escande D, Schumacher CA, et al. Potassium accumulation in the globally ischemic mammalian heart. A role for the ATP-sensitive potassium channel. Circ Res 1990;67:835–843.

[20] Yan GX, Kléber AG. Changes in extracellular and intracellular pH in ischemic rabbit papillary muscle. Circ Res 1992;71:460–470.

[21] Yatani A, Brown AM, Akaike N. Effect of extracellular pH on sodium current in isolated, single rat ventricular cells. J Membr Biol 1984;78:163–168.

[22] Kagiyama Y, Hill JL, Gettes LS. Interaction of acidosis and increased extracellular potassium on action potential characteristics and conduction in guinea pig ventricular muscle. Circ Res 1982;51:614–623.

[23] Irisawa H, Sato R. Intra- and extracellular actions of proton on the calcium current of isolated guinea pig ventricular cells. Circ Res 1986;59:348–355.

[24] Grant AO, Strauss LJ, Wallace AG, Strauss HC. The influence of pH on the electrophysiological effects of lidocaine in guinea pig ventricular myocardium. Circ Res 1980;47:542–550.

[25] Skinner RB Jr., Kunze DL. Changes in extracellular potassium activity in response to decreased pH in rabbit atrial muscle. Circ Res 1976;39:678–683.

[26] Noma A. ATP-regulated $K^+$ channels in cardiac muscle. Nature 1983;305:147–148.

[27] Shaw RM, Rudy YR. Electrophysiological changes of ventricular tissue under ischemic conditions: a simulation study. Comp Cardiol 1994;16:641–644.

[28] Nichols CG, Ripoll C, Lederer WJ. ATP-sensitive potassium channel modulation of the guinea pig ventricular action potential and contraction. Circ Res 1991;68:280–287.

[29] Weiss JN, Venkatesh N, Lamp ST. ATP-sensitive $K^+$ channels and cellular $K^+$ loss in hypoxic and ischaemic mammalian ventricle. J Physiol (Lond) 1992;447:649–673.

[30] Lederer WJ, Nichols CG, Smith GL. The mechanism of early contractile failure of isolated rat ventricular myocytes subjected to complete metabolic inhibition. J Physiol (Lond) 1989;413:329–349.

[31] Han J, So I, Kim EY, Earm YE. ATP-sensitive potassium channels are modulated by intracellular lactate in rabbit ventricular myocytes. Pflugers Arch 1993;425:546–548.

[32] Kakei M, Noma A, Shibasaki T. Properties of adenosine-triphosphate-regulated potassium channels in guinea-pig ventricular cells. J Physiol (Lond) 1985;363:441–462.

[33] Noma A, Shibasaki T. Membrane current through adenosine-triphosphate-regulated potassium channels in guinea-pig ventricular cells. J Physiol (Lond) 1985;363:463–480.

[34] Ohya Y, Sperelakis N. ATP regulation of the slow calcium channels in vascular smooth muscle cells of guinea pig mesenteric artery. Circ Res 1989;64:145–154.

[35] Rush S, Larsen H. A practical algorithm for solving dynamic membrane equations. IEEE Trans Biomed Eng 1978;25:389–392.

[36] Gettes LS, Buchanan JW Jr., Saito T, Kagiyama Y, Oshita S, Fujino T. Studies concerned with slow conduction. In: Zipes DP, Jalife J, editors. Cardiac electrophysiology and arrhythmias. Orlando, FL: Grune and Stratton, 1985:81–87.

[37] Beeler GW, Reuter H. Reconstruction of the action potential of ventricular myocardial fibres. J Physiol (Lond) 1977;268:177–210.

[38] Nichols CG, Lederer WJ. Adenosine triphosphate-sensitive potassium channels in the cardiovascular system. Am J Physiol 1991;261:H1675–H1686.

[39] Yan GX, Yamada KA, Kléber AG, McHowat J, Corr PB. Dissociation between cellular $K^+$ loss, reduction in repolarization time, and tissue ATP levels during myocardial hypoxia and ischemia. Circ Res 1993;72:560–570.

[40] Cranefield PF, Wit AL, Hoffman BF. Conduction of the cardiac impulse. 3. Characteristics of very slow conduction. J Gen Physiol 1972;59:227–246.

[41] Gilmour RF Jr., Zipes DP. Electrophysiological response of vascularized hamster cardiac transplants to ischemia. Circ Res 1982;50:599–609.

[42] Cardinal R, Janse MJ, Van Eeden I, Werner G, d'Alnoncourt CN, Durrer D. The effects of lidocaine on intracellular and extracellular potentials, activation, and ventricular arrhythmias during acute regional ischemia in the isolated porcine heart. Circ Res 1981;49:792–806.

[43] Nichols CG, Lederer WJ. The regulation of ATP-sensitive K channel activity in intact and permeabilized rat ventricular myocytes. J Physiol 1990;423:91–110.

[44] Allen DG, Morris PG, Orchard CH, Pirolo JS. A nuclear magnetic resonance study of metabolism in the ferret heart during hypoxia and inhibition of glycolysis. J Physiol (Lond) 1985;361:185–204.

[45] Elliott AC, Smith GL, Allen DG. Simultaneous measurements of action potential duration and intracellular ATP in isolated ferret hearts exposed to cyanide. Circ Res 1989;64:583–591.

[46] Venkatesh N, Lamp ST, Weiss JN. Sulfonylureas, ATP-sensitive $K^+$ channels, and cellular $K^+$ loss during hypoxia, ischemia, and metabolic inhibition in mammalian ventricle. Circ Res 1991;69:623–637.

[47] Faivre JF, Findlay I. Action potential duration and activation of ATP-sensitive potassium current in isolated guinea-pig ventricular myocytes. Biochim Biophys Acta 1990;1029:167–172.

[48] Philipson KD, Bersohn MM, Nishimoto AY. Effects of pH on $Na^+$–$Ca^{2+}$ exchange in canine cardiac sarcolemmal vesicles. Circ Res 1982;50:287–293.

[49] Doering AE, Lederer WJ. The mechanism by which cytoplasmic protons inhibit the sodium–calcium exchanger in guinea-pig heart cells. J Physiol 1993;466:481–499.

[50] Le Guennec JY, Noble D. Effects of rapid changes of external $Na^+$ concentration at different moments during the action potential in guinea-pig myocytes. J Physiol 1994;478(3):493–504.

[51] Sano T, Hiraoka M, Sawanobori T. Effects of anoxia and metabolic inhibitors on reactivation of the fast sodium system. In: Kobayashi T, Sano T, Dhalla NS, editors. Recent advances in studies on cardiac structure and metabolism, Vol. 11. Baltimore: University Press, 1978:79–83.

[52] Cascio WE, Yan GX, Kléber AG. Early changes in extracellular potassium in ischemic rabbit myocardium. The role of extracellular carbon dioxide accumulation and diffusion. Circ Res 1992;70:409–422.

[53] Sato T, Kiyosue T, Arita M. Inhibitory effects of palmitoylcarnitine and lysophosphatidylcholine on the sodium current of cardiac ventricular cells. Pflugers Arch 1992;420:94–100.

[54] Wu J, Corr PB. Influence of long-chain acylcarnitines on voltage-dependent calcium current in adult ventricular myocytes. Am J Physiol 1992;263:H410–H417.

[55] Sato R, Noma A, Kurachi Y, Irisawa H. Effects of intracellular acidification on membrane currents in ventricular cells of the guinea pig. Circ Res 1985;57:553–561.

[56] Harvey RD, Ten Eick RE. On the role of sodium ions in the regulation of the inward-rectifying potassium conductance in cat ventricular myocytes. J Gen Physiol 1989;94:329–348.

[57] Whalley DW, Wendt DJ, Grant AO. Electrophysiological effects of acute ischemia and reperfusion and their role in the genesis of cardiac arrhythmias. In: Podrid PJ, Kowey PR, editors. Cardiac arrhythmias: mechanisms, diagnosis, and management. Baltimore: Williams and Wilkins, 1994:109–130.

[58] Tani M, Neely JR. Role of intracellular $Na^+$ in $Ca^{2+}$ overload and depressed recovery of ventricular function of reperfused ischemic rat hearts. Possible involvement of $H^+$–$Na^+$ and $Na^+$–$Ca^{2+}$ exchange. Circ Res 1989;65:1045–1056.

[59] Steenbergen C, Murphy E, Watts JA, London RE. Correlation between cytosolic free calcium, contracture, ATP, and irreversible ischemic injury in perfused rat heart. Circ Res 1990;66:135–146.

[60] Maruyama T, Cascio WE, Knisley SB, Buchanan J, Gettes LS. Effects of ryanodine and BAY K 8644 on membrane properties and conduction during simulated ischemia. Am J Physiol 1991;261:H2008–H2015.